# Friction effects and clogging in a cellular automaton model for pedestrian dynamics

Ansgar Kirchner,* Katsuhiro Nishinari,† and Andreas Schadschneider‡
*Institut für Theoretische Physik, Universität zu Köln D-50937 Köln, Germany*
(Dated: February 1, 2008)

We investigate the role of conflicts in pedestrian traffic, i.e. situations where two or more people try to enter the same space. Therefore a recently introduced cellular automaton model for pedestrian dynamics is extended by a friction parameter $\mu$. This parameter controls the probability that the movement of *all* particles involved in a conflict is denied at one time step. It is shown that these conflicts are not an undesirable artefact of the parallel update scheme, but are important for a correct description of the dynamics. The friction parameter $\mu$ can be interpreted as a kind of internal local pressure between the pedestrians which becomes important in regions of high density, ocurring e.g. in panic situations. We present simulations of the evacuation of a large room with one door. It is found that friction has not only quantitative effects, but can also lead to qualitative changes, e.g. of the dependence of the evacuation time on the system parameters. We also observe similarities to the flow of granular materials, e.g. arching effects.

PACS numbers: 45.70.Vn, 02.50.Ey, 05.40.-a

## I. INTRODUCTION

Methods of physics and modern computer science have been used successfully for the investigation of vehicular traffic problems for a long time [1, 2, 3]. Also pedestrian dynamics has attracted some attention in recent years [4] and many interesting collective effects and self-organisation phenomena have been observed (for an overview see [2, 3, 4, 5]).

One topic which has not been studied intensively up to now (see, however, [6]) is the relevance of local conflicts in pedestrian traffic. A conflict indicates a situation in which two or more people try to enter the same space in one timestep. Obviously this is a real two-dimensional effect which has no counterpart in (directed) one-dimensional vehicular traffic. These conflicts are local phenomena which can have a strong influence on global quantities like evacuation times and flows in the presence of bottlenecks. Typical examples where conflicts become important are situations with clogging and stucking encountered in crowds of panicing pedestrians, e.g. near intersections and bottlenecks. In real life this often leads to very dangerous situations and injuries or even fatalities during evacuations. From a physics point of view these phenomena are related to flow properties of granular materials [7, 8, 9, 10, 11, 12, 13].

Depending on the choice of parameters, the cellular automaton (CA) model introduced in [14, 15, 16] is able to reproduce many of the observed collective effects of pedestrian dynamics, i.e. panicing and herding behaviour [17]. In this paper the model is extended by a friction parameter $\mu$, which allows an improved description of clogging and stucking phenomena of pedestrians. It will be shown that conflicts and friction are responsible for several interesting effects which become especially relevant in high density situations, e.g. during evacuation processes, and that they are important for a correct reproduction of the dynamics. We start with a short summary of the model's basic concepts and its update rules.

## II. BASIC PRINCIPLES OF THE MODEL

The model considered here is a CA where the space is discretized into small cells which can either be empty or occupied by exactly one pedestrian. Each of these pedestrians can move to one of its unoccupied neighbour cells (see fig. 1) at each discrete time step $t \to t+1$ according to certain transition probabilities. The probabilities

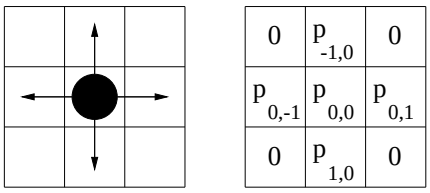


FIG. 1: Definition of the transition probabilities $p_{ij}$.

are given by the interaction with two discrete *floor fields*, $D$ and $S$ [14, 15, 16, 17]. The field strengths $D_{ij}$ and $S_{ij}$ at site $(i,j)$ are interpreted as number of $D$- and $S$-particles, respectively, present at that site. The two fields determine the transition probability in such a way that a particle movement in the direction of higher fields becomes more likely.

The dynamic floor field $D$ represents a virtual trace left by *moving* pedestrians. Similar to the process of chemotaxis [18, 19] used by some insects for communication, this trace has its own dynamics, namely diffusion

*Electronic address: aki@thp.uni-koeln.de
†Electronic address: kn@thp.uni-koeln.de; Permanent address: Department of Applied Mathematics and Informatics, Ryukoku University, Shiga, Japan (email: knishi@rins.ryukoku.ac.jp)
‡Electronic address: as@thp.uni-koeln.de

and decay. Two parameters, $\alpha \in [0,1]$ and $\delta \in [0,1]$, control the broadening and dilution of the trace. Every moving pedestrian creates a $D$-particle at its origin cell. Since there is no restriction of the maximal number of $D$-particles at a site, $D$ can be regarded as a *bosonic field*.

The static floor field $S$, on the other hand, does not change in time. It reflects the surrounding geometry and e.g. specifying attractive space regions. In the case of the evacuation processes considered here, the static floor field describes the shortest distance to an exit door. $S$ is calculated for each lattice site using some distance metric. The field value increases in the direction of the exit such that it is largest for door cells. An explicit construction of $S$ can be found in [17, 20].

The floor fields are used to translate a long-ranged spatial interaction into a local interaction, but with memory, similar to the phenomenon of chemotaxis in biology. The only other model which so far reproduces all observed collective effects of pedestrian flow, the social-force model [21], uses exponentially decaying repulsive forces between pedestrians. In contrast, in our approach the interaction is local and attractive. However, pedestrians do not interact with the density, but with the velocity density created by the other particles.

### A. Update rules

The update rules of the full model, including the interaction with the two floor fields, have the following structure:

1. The dynamic floor field $D$ is modified according to its diffusion and decay rules [14], controlled by the parameters $\alpha$ and $\delta$. In each time step of the simulation each single boson of the whole dynamic field $D$ decays with the probability $\delta$ and diffuses with the probability $\alpha$ to one of its neighbouring cells.

2. For each pedestrian, the transition probabilities $p_{ij}$ for a move to an unoccupied neighbour cell $(i,j)$ (fig. 1) are determined by the local dynamics and the two floor fields. The values of the fields $D$ and $S$ are weighted with two sensitivity parameters $k_S \in [0,\infty[$ and $k_D \in [0,\infty[$. This yields

$$p_{ij} = N \exp(k_D D_{ij}) \exp(k_S S_{ij})(1-n_{ij})\xi_{ij}\,, \qquad (1)$$

with the occupation number $n_{ij} = 0, 1$, the obstacle number

$$\xi_{ij} = \begin{cases} 0 & \text{for forbidden cells (e.g. walls)} \\ 1 & \text{else} \end{cases} \qquad (2)$$

and the normalization

$$N = \left[ \sum_{(i,j)} e^{k_D D_{ij}} e^{k_S S_{ij}} (1-n_{ij})\xi_{ij} \right]^{-1} . \qquad (3)$$

3. Each pedestrian chooses randomly a target cell based on the transition probabilities $p_{ij}$ determined by (1).

4. Conflicts arising by any two or more pedestrians attempting to move to the same target cell are resolved by a probabilistic method. The pedestrians which are allowed to move execute their step. The explicit procedure of conflict resolution will be described in detail in section III.

5. $D$ at the origin cell $(i,j)$ of each *moving* particle is increased by one: $D_{ij} \to D_{ij} + 1$.

The above rules are applied to all pedestrians at the same time (parallel update). This introduces a timescale of about 0.3 sec/timestep [14].

## III. RESOLUTION OF CONFLICTS

Due to the use of parallel dynamics it is possible that two or more particles choose the same destination cell in Step 3 of the update procedure. Such situations will be called *conflicts*. At first it appears that conflicts are undesirable effects which reduce the efficiency of simulations and should therefore be avoided by choosing a different update scheme. We will show in the following that this is not the case and that conflicts are important for a correct description of the physics of crowd dynamics.

### A. Conflicts without friction

In [14, 17] conflicts between pedestrians were solved in the following way: whenever $m > 1$ particles share the same target cell, one ($l \in \{1, \ldots, m\}$) is chosen to move while its rivals for the same target keep their position. There are two main ways to decide which particle $l$ is allowed to move:

1. According to the relative probabilities with which each particle chooses its target cell, i.e. the probability for particle $l$ to move is $p_{ij}^{(l)} / \sum_{s=1}^{m} p_{ij}^{(s)}$.

2. All particles move with the same probability $\frac{1}{m}$.

The observed behaviour has been shown to be quite robust and does not depend on the details of the conflict resolution [14].

### B. Introduction of the friction parameter $\mu$

We now extend the basic model by a new friction parameter $\mu \in [0,1]$, in order to describe clogging and stucking effects between the pedestrians. Whenever two or more pedestrians try to attempt to move to the same target cell, the movement of *all* involved particles is denied with the probability $\mu$, i.e. all pedestrians remain

at their site (see fig. 2). This means that with probability $1-\mu$ one of the individuals moves to the desired cell. Which particle actually moves is then determined by the rules for the resolution of conflicts as described in Sec. III A. Note that for vanishing friction $\mu = 0$ we recover the dynamics studied in [14, 15, 16, 17].

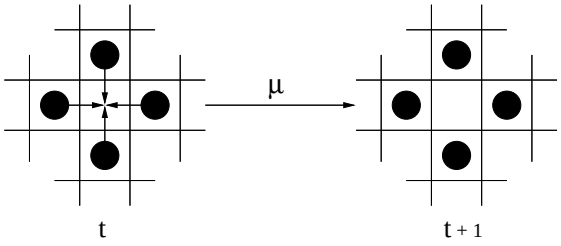


FIG. 2: Refused movement (for $m = 4$) due to the friction parameter $\mu$.

The friction parameter might be interpreted as the effect of a moment of hesitation: Pedestrians in conflict situations slow down or hesitate for a short moment when trying to resolve the conflict. This reduces on average the velocities of all involved particles.

With the above definition of $\mu$ and the extended update rule it is easy to see that $\mu$ works as some kind of local pressure between the pedestrians. If $\mu$ is high, the pedestrians handicap each other trying to reach their desired target sites. As we will see, this local effect can have enormous influence on macroscopic quantities like flow and evacuation time. We like to point out that friction as introduced here does not reduce the velocity of a freely moving particle. Its effects only show up in local *interactions*.

As one can see it is necessary for such kind of investigations to use a parallel update in the model. Any other form of random or ordered sequential update will disguise the real number of arising conflicts between the pedestrians in the system.

## IV. SIMULATIONS AND RESULTS

In the following we describe results of simulations for a typical situation, i.e. the evacuation of a large room (e.g. in case of fire). In [17] it is shown that by variation of the sensitivity parameters $k_S$ and $k_D$ (see Sec. II A) three main regimes for the behaviour of the particles can be distinguished. For strong coupling $k_S$ and very small coupling $k_D$ we find an *ordered regime* where particles only react to the static floor field. The behaviour then is in some sense deterministic. The *disordered regime* characterized by strong coupling $k_D$ and weak coupling $k_S$ leads to a maximal value of the evacuation time $T$. Here the behaviour is typical for panic situations. Between these two regimes an *cooperative regime* [22] exists where the combination of interactions with the static and the dynamic floor fields minimizes the evacuation time. Fig. 3 shows a schematical phase diagram in the space of the couplings $k_S$ and $k_D$.

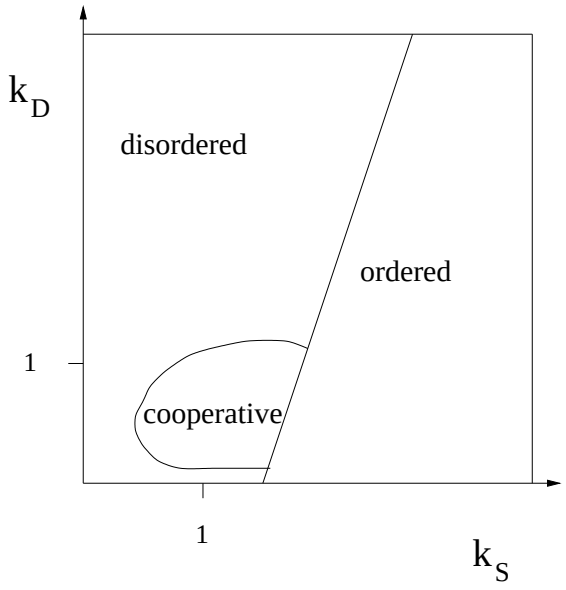


FIG. 3: Schematic phase diagram.

Here we want to focus on the influence of the friction parameter $\mu$ on the evacuation times in the three main regimes. As we will see the influence of $\mu$ is strongest in the ordered regime. This will lead to a new interpretation of this regime.

We consider a grid of size $63 \times 63$ sites with a small exit of one cell in the middle of one wall. The particles are initially distributed randomly and try to leave the room. The only information they get is through the floor fields. The strength of the static floor field at a site $(i, j)$ is inversely proportional to the distance of $(i, j)$ from the exit measured using the metric described in [17]. Fig. 4 shows a typical stage of the dynamics for an initial particle density of $\rho = 0.3$, i.e. 1116 particles. A typical half-circle jamming configuration in front of the door develops.

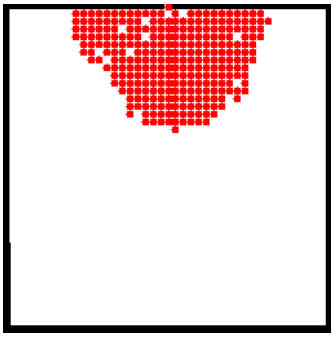

FIG. 4: Typical middle stage of the dynamics of an evacuation.

### A. Influence of $\mu$ and $\rho$

First we look at the averaged evacuation times $T$ in the three main regimes, in dependence of the particle density $\rho$ and the friction parameter $\mu$. All evacuation times are averaged over 500 samples and measured in update steps. Figs. 5 and 6 show the influence of a varying $\mu$ parameter on the three regimes for the low density $\rho = 0.03$ and the high density $\rho = 0.3$.

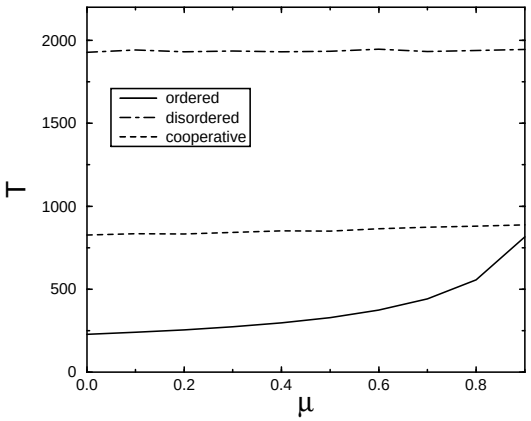


FIG. 5: Average evacuation times $T$ for a large room in dependence of the friction parameter $\mu$ for the low density $\rho = 0.03$.

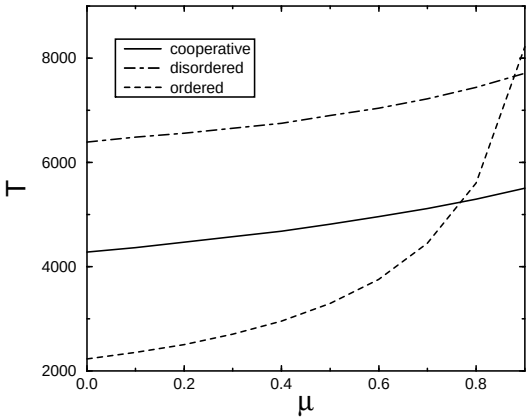


FIG. 6: Same as fig. 5, but for a higher density of $\rho = 0.3$.

In the low density regime, $\rho = 0.03$ (fig. 5), increasing $\mu$ has only a very weak effect on the evacuation times of the disordered and the cooperative regime. Here the pedestrians move almost independently of each other so that conflict situations, even close to the door, are rare since almost no jamming occurs. The behaviour is different in the ordered regime. All particles find the shortest way to the exit. Even for low densities they will form a jam in front of the door after a short time. But since these jams are small, the evacuation time increases only for large friction parameters $\mu > \frac{1}{2}$.

The behaviour is different in the high density regime $\rho = 0.3$ (fig. 6). One finds a weak increase of the evacuation time in the disordered and cooperative regime for high $\mu$ values ($\mu > 0.6$). Even if the particles are not packed close together in front of the door, they form a cue and hinder each other. Increasing $\mu$ leads to a sharp increase of the evacuation time in the ordered regime which first becomes larger than that in the cooperative regime and finally exceeds even that in the disordered regime. In fact it diverges for $\mu \longrightarrow 1$. This behaviour can be understood from the microscopic configurations occuring. A short time after the start of the evacuation nearly all particles of the system are forming a big jam in front of the door. In this large density region many conflicts occur and for large values of $\mu$ the outflow is strongly surpressed. Here the pressure between the pedestrians becomes so strong that any motion is almost impossible. Such a behaviour has been observed in panic situations and also in simulations using the social-force model [6]. It will be discussed in more detail in Sec. IV B.

These results are supported by figs. 7 and 8 which show the influence of an increased density $\rho$ for fixed values of $\mu$ on the evacuation times. In the disordered regime even

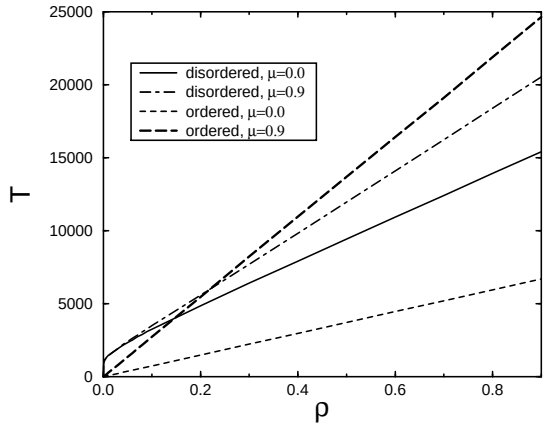


FIG. 7: Density-dependence of the evacuation time in the ordered and disordered regime for $\mu = 0.9$.

the influence of the large value $\mu = 0.9$ is only visible for higher densities ($\rho > 0.1$). The cooperative regime shows a similar behaviour. In contrast, in the ordered regime even for very small densities $\rho$ the influence of the high value $\mu = 0.9$ is very strong (fig. 7). This is supported by fig. 8, where the relative time differences for the two values $\mu = 0$ and $\mu = 0.9$ for all three regimes are shown. Here the very strong increase of the relative time difference in the ordered regime after a very small

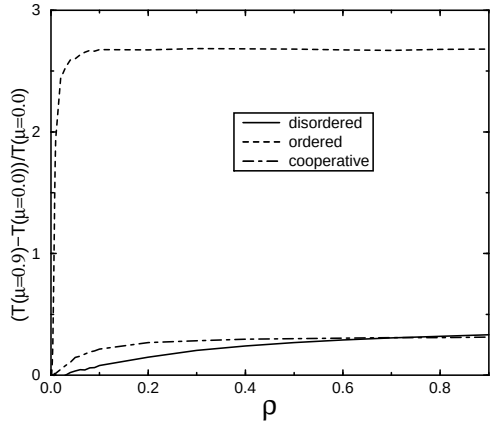


FIG. 8: Relative time difference of the evacuation times for $\mu = 0$ and $\mu = 0.9$ in the three regimes.

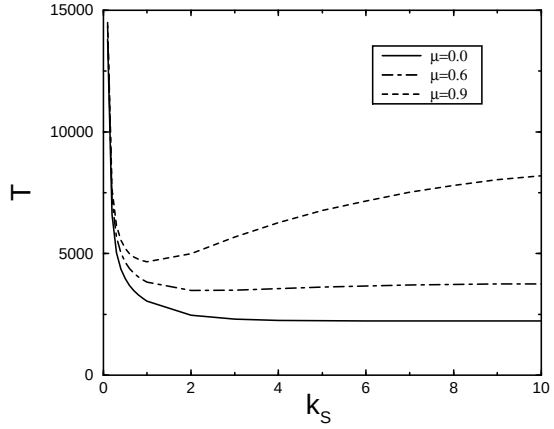


FIG. 9: Evacuation time as function of the sensitivity parameter $k_S$ for different $\mu$ values ($k_D = 0$, $\rho = 0.3$).

density of $\rho = 0.003$ is remarkable. After this increase the relative time difference remains almost constant.

### B. Reinterpretation of the ordered phase

The introduction of the friction parameter $\mu$ allows an improved interpretation of the ordered regime, i.e. the case of strong coupling ($k_S > 3$) to the static field $S$ and weak coupling to dynamic field $D$. This regime is almost deterministic, with pedestrians moving straight towards the exit on the shortest path. Now an increased $\mu$ value introduces a negative interaction between the particles into the system, i.e. the pedestrians hinder each other due to strong competition for the unoccupied target sites near the exit. So a strong coupling to $S$ together with a high $\mu$ value, which works as an internal local pressure between the particles, describes a typical panic situation, where an ordered outflow is inhibited due to local conflicts near bottlenecks or doors, resulting in strongly increased evacuation times (such situations are well known from emergency evacuations due to fire or other reasons in sports arenas or passenger vessels). This can be seen in fig. 9, where the influence of an increased coupling strength to $S$ for fixed $\mu$ is shown. For $k_S \longrightarrow 0$ the particles perform a pure random walk and the evacuation times are very large and almost independent of $\mu$. In this situation conflicts between the particles are not very important for the dynamics. In contrast, for $k_S \longrightarrow \infty$ they choose the shortest way to the exit. Since for $\mu = 0$ there is no internal pressure between the particles the evacuation time is minimal. However, for $\mu \longrightarrow 1$ the number of unsolved conflicts increases with $k_S$ due to the strong jamming at the exit. This results in stucking and clogging phenomena and highly increased evacuation times. For very high $\mu$ values ($\mu = 0.9$ in fig. 9) one finds a *minimal* evacuation time for an intermediate coupling ($k_S \approx 1$). This means that a larger $k_S$, which implies a larger average velocity of freely moving pedestrians, leads to larger evacuation times. This collective phenomenon is very similar to the faster-is-slower effect [5, 6]. Note that a similar minimum is characteristic for the cooperative regime. However, there local minima have been observed as a function of the coupling $k_D$ to the dynamic floor instead of $k_S$ [17].

### C. Time evolution of an evacuation

In the following we look at the time evolution of an evacuation, i.e. the number of people who left the room at a certain time stage. Figs. 10 and 11 show the time dependence of the number of evacuated persons for all three regimes and different $\mu$ values for a high density $\rho = 0.3$. The curves show a nearly linear increase since the very high initial density leads to strong clustering at the door already at the beginning of the evacuation. The evacuation times are strongly increased due to the large value $\mu = 0.9$. This effect is again strongest in the ordered phase. For $\mu = 0$ the corresponding evacuation time is the smallest whereas for $\mu = 0.9$ it becomes the largest one of all regimes. At the end of the evacuations, when most of the particles have left the room, the gradient of the curves becomes rather small.

Because of the averaging over many samples the curves are very smooth. To have an impression of the evolution of one single evacuation and of the variance of evacuation times, fig. 12 shows the averaged curves envelloped by the curves with the minimal and the maximal evacuation time of the whole sample for the ordered phase and three $\mu$ values. For $\mu = 0$ the evacuation process is nearly deterministic in the ordered regime and the fluctuations

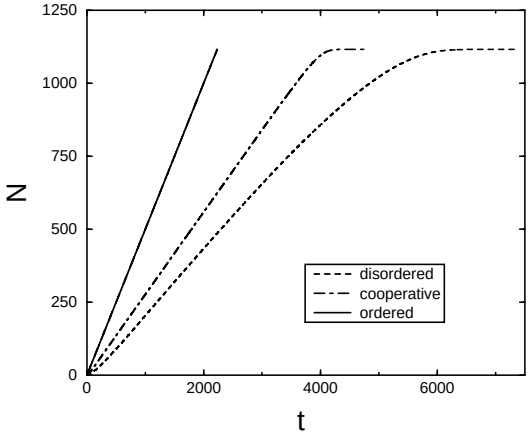


FIG. 10: Evacuated persons $N$ in dependence of time $t$ for all three regimes; $\rho = 0.3$ and $\mu = 0.$

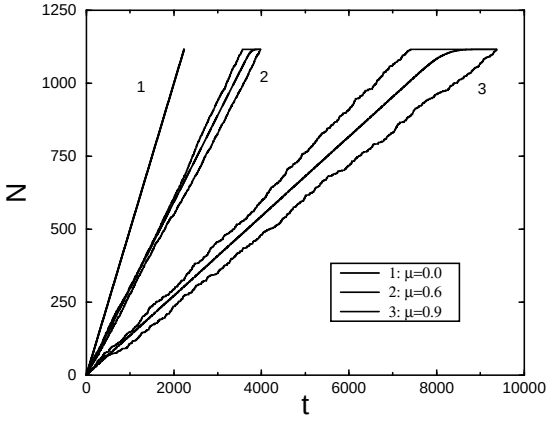


FIG. 12: Evacuated persons as function of time for the ordered regime for density $\rho = 0.3$. Shown are the averaged, longest and shortest evacuation process for three $\mu$ values.

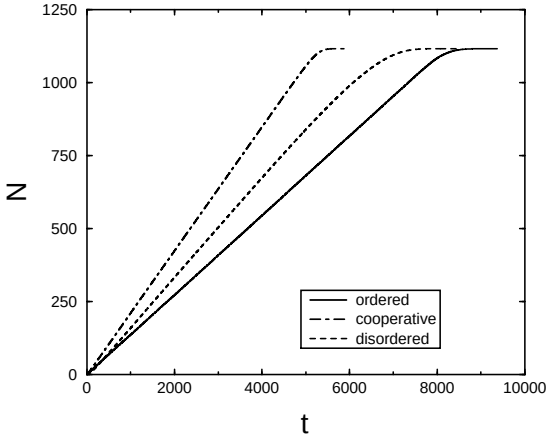


FIG. 11: Evacuated persons in dependence of time for all three regimes; $\rho = 0.3$ and $\mu = 0.9$.

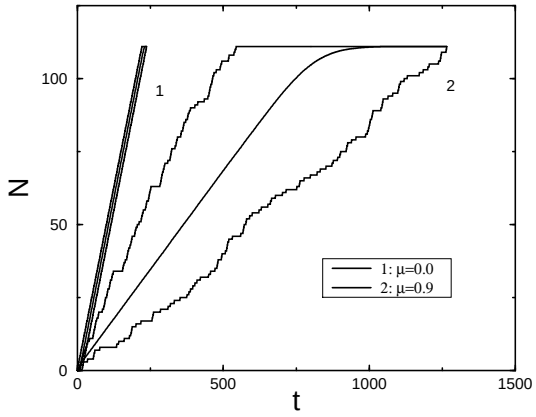


FIG. 13: Evacuated persons in dependence of time for the ordered regime; averaged, longest and shortest evacuation process for two $\mu$ values ($\mu = 0$ and $\mu = 0.9$) and density $\rho = 0.03$.

(due to the random initial conditions and the dynamics) are very small. With increasing $\mu$ values the internal pressure is increased and the envelloping curves differ clearly from the averaged curves.

In figs. 13 and 14 again the averaged curves together with the extremals are shown for the two densities $\rho = 0.03$ (fig. 13) and $\rho = 0.003$ (fig. 14) and the two friction parameters $\mu = 0$ and $\mu = 0.9$. Here the same effects as for $\rho = 0.3$ can be seen, but much clearer.

The time evolution of one single sample exhibits an interesting dynamics. In figs. 12–14 small plateaus can be observed where over short time periods no persons leave the room. This irregular behaviour is well-known from granular flow and is typical for clogging situations [7, 8, 9, 10, 11, 12, 13]. The plateaus are formed stochastically and can therefore not be observed after averaging over various samples (figs. 10, 11).

Note that also the variance of the evacuation time increases strongly with $\mu$. Fig. 13 shows that the average evacuation time $T$ is not always a meaningful quantity for safety estimates since the variance can become quite large. For the very small density $\rho = 0.003$ the gradient of the curve is rather flat at the beginning of the evacuation (fig. 14). Here there are only few particles in the system and no cue is formed near the exit.

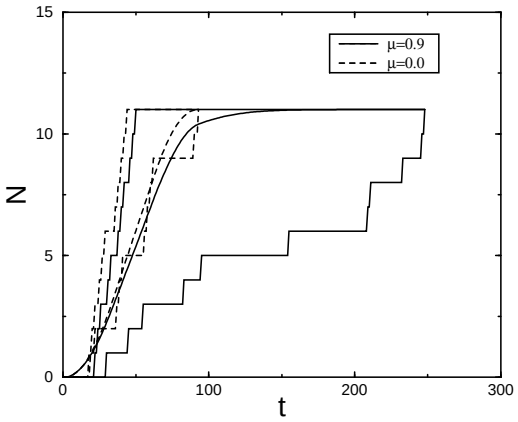


FIG. 14: Evacuated persons in dependence of time for the ordered regime; averaged, longest and shortest evacuation process for two $\mu$ values ($\mu = 0$, $\mu = 0.9$) and density $\rho = 0.003$.

### D. Mean-field approximation for the ordered regime

As we have seen in Sec. IV C the curve of the number of evacuated persons $N(t)$ grows almost linearly in the ordered regime, especially for high densities $\rho$. For this regime we now calculate approximatively the $\mu$-dependence of this curve, i.e. $N = N(t, \mu)$.

As explained earlier, in the ordered regime after a short time a big jam forms at the door due to the strong coupling to the static field $S$. Fig. 15 shows a typical local configuration in front of the exit. Generically, 3-particle

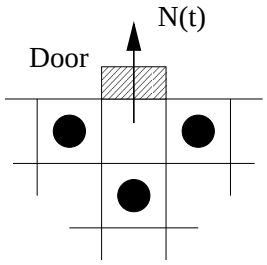


FIG. 15: Typical configuration in front of the door in the ordered regime.

conflicts over the unoccupied lattice site in front of the door occur. At time $t$, with probability $1-\mu$ one of these particles is able to move. In the next time step $t+1$ this particle will escape through the door with probability 1. Neglecting conflicts elsewhere in the system, because of the big jam in front of the door the configuration shown in fig. 15 will be restored at time $t+2$. Therefore, repeating the above sequence a typical representation of the time evolution of $N(t)$ is shown in fig. 16.

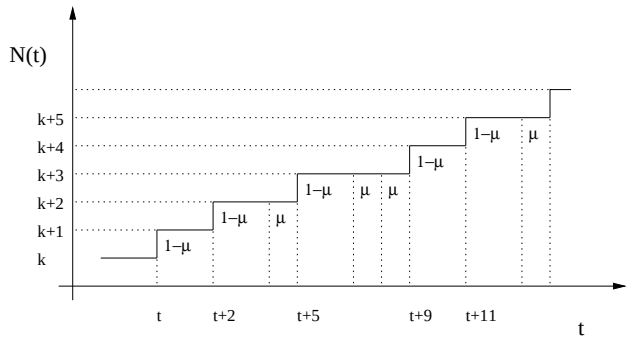


FIG. 16: An example for the time evolution of the number of evacuated persons.

Using simple combinatorics, the expectation value of $N(t)$ can be written as

$$\langle N(t)\rangle = \frac{1}{C}\sum_{n=0}^{[t/2]} n \left( \begin{array}{c} t-n \\ n \end{array} \right) (1-\mu)^n \mu^{t-2n}, \qquad (4)$$

where $C$ is the normalization factor defined by

$$\begin{aligned} C(t) &= \sum_{n=0}^{[t/2]} \left( \begin{array}{c} t-n \\ n \end{array} \right) (1-\mu)^n \mu^{t-2n} \\ &= \mu^t \sum_{n=0}^{[t/2]} \left( \begin{array}{c} t-n \\ n \end{array} \right) \left( \frac{1-\mu}{\mu^2} \right)^n \\ &= \frac{1-(\mu-1)^{t+1}}{2-\mu}. \end{aligned} \qquad (5)$$

In the last step we have used the identity (A8) which is derived in Appendix A. Due to (4) and (5), $\langle N(t)\rangle$ is related to $C$ by the equation

$$\frac{d}{d\mu}C = \frac{t}{\mu}\, C + \frac{\mu-2}{\mu(1-\mu)}\, \langle N(t)\rangle\, C \qquad (6)$$

or

$$\langle N(t)\rangle = \frac{\mu(1-\mu)}{\mu-2}\left( \frac{d}{d\mu}\log C - \frac{t}{\mu} \right). \qquad (7)$$

Finally an analytical expression for $\langle N(t)\rangle$ is obtained as

$$\begin{aligned} \langle N(t)\rangle = &\frac{\mu-1}{(\mu-2)^2}\cdot \\ &\left( \mu(1+t) - 2t - \frac{(\mu-2)(\mu-1)^t\mu(1+t)}{(\mu-1)^{t+1}-1} \right). \end{aligned} \qquad (8)$$

Asymptotically, (8) implies for large times

$$\langle N(t)\rangle \sim \frac{1-\mu}{2-\mu}\cdot t \quad \text{as } t\to\infty\,, \qquad (9)$$

i.e. a linear behaviour as observed in simulations for the ordered regime. This expression is also consistent with

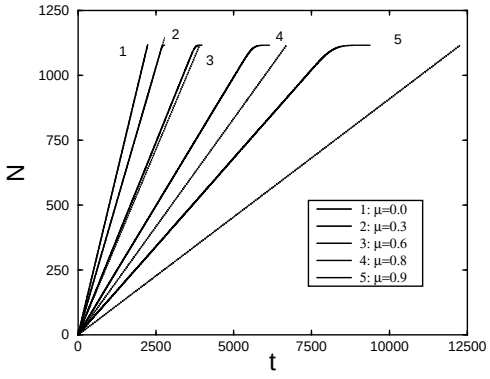


FIG. 17: Evacuated persons in dependence of time for the ordered regime; comparison of the numerical results with the analytical approximation (9) for the density $\rho = 0.3$.

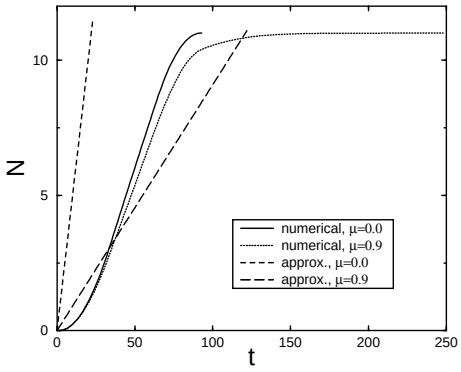


FIG. 18: Time-dependence of the number of evacuated persons for the ordered regime; comparison of the numerical results with the analytical approximation (9) for the density $\rho = 0.003$.

the fact that $T \to \infty$ for $\mu \to 1$. From fig. 17 we see that the analytical approximation (9) for $\langle N(t) \rangle$ is very good for high densities ($\rho = 0.3$) and friction parameter values $\mu \leq 0.6$. However, for very high parameter values ($\mu \geq 0.8$) the agreement is not satsifactory. Here the assumption that a typical local configuration looks like that in fig. 15 no longer holds. The observed flow is underestimated since the large friction parameter $\mu$ is responsible for a flow reduction through conflicts occuring away from the door. Therefore particles are not so dense-packed at the exit (compared to the situation at smaller $\mu$-values) which leads to an effective reduction of conflicts.

In the low density regime $\rho = 0.03$ (not shown in the figure) the approximation again gives satisfactory agreement for $\mu \leq 0.6$. Only in the region of very low densities (e.g. $\rho = 0.003$, see fig. 18) strong deviations can be observed for all $\mu$ values. In this case there are only very few particles in the system, not hindering each other. In most cases they reach the exit independently and the evacuation time essentially depends on the diameter of the room (or the average walking length) rather than on the number of particles in the system.

### E. Number of conflicts during evacuation

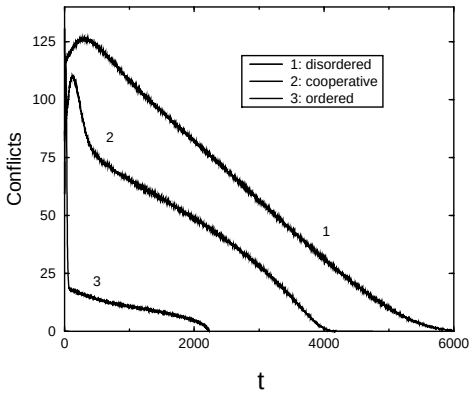


FIG. 19: Number of conflicts in dependence of time $t$ for all three regimes ($\rho = 0.3$ and $\mu = 0$).

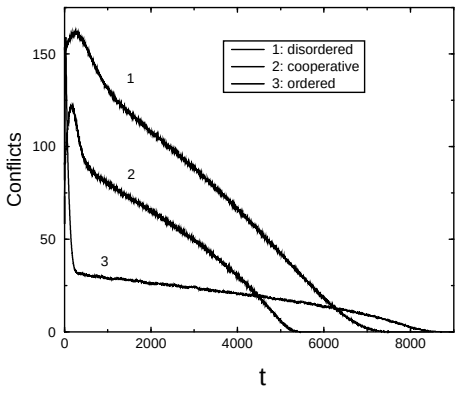


FIG. 20: Number of conflicts in dependence of time for all three regimes ($\rho = 0.3$, $\mu = 0.9$).

Next we investigate the time evolution of the number of conflicts arising during an evacuation process. Figs. 19 and 20 show the number of conflicts in dependence of time for all three regimes in the high density case $\rho = 0.3$. The maximal number of conflicts occurs for all regimes and $\mu$ values shortly after the beginning of the evacuation. The number of conflicts is always largest in the

disordered regime. As argued earlier here the motion resembles a random walk. Since there are many particles in the system most of them will compete for empty sites with other particles crossing their path anywhere in the room. In the ordered regime all pedestrians gather around the exit quickly with most of them standing in the cue without competing [23]. Even though the number of conflicts is smallest in the ordered regime, the influence of the friction parameter on the evacuation time is strongest. The reason behind this is that nearly all conflicts take place in front of the door. Therefore they have a direct effect on the outflow which is reduced considerably. Conflicts arising away from the exit do not have a direct influence on the evacuation time. In fact they can even lead to an increased outflow because they might surpress clogging at the door (see Sec. IV F).

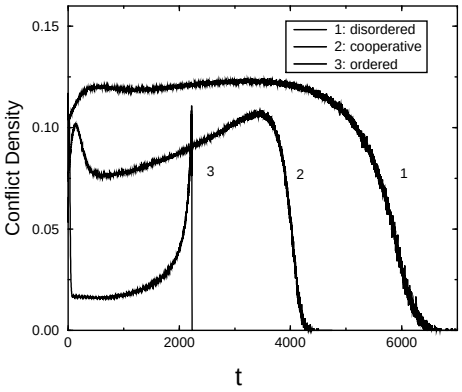


FIG. 21: Conflict density in dependence of time $t$ for all three regimes ($\rho = 0.3$ and $\mu = 0$).

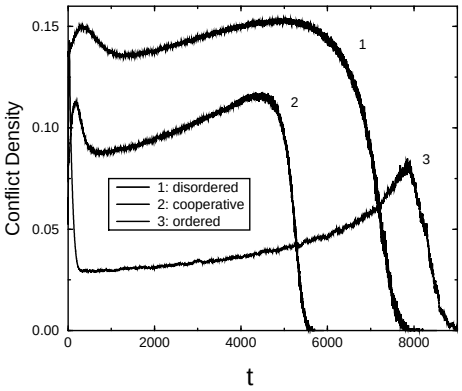


FIG. 22: Same as fig. 21, but with $\rho = 0.3$ and $\mu = 0.9$.

In figs. 21 and 22 the corresponding conflict densities, i.e. the number of conflicts divided by the number of particles inside the room, are shown. In fig. 21 one can see a very strong increase of the conflict density in the ordered regime at the end of the evacuation for $\mu = 0$. During most of the time of the evacuation the majority of particles are forming a big jam and do not contribute to the conflict density. At the end of the evacuation the jam nearly is dissolved and only few particles are left in the room near the exit conflicting about the unoccupied sites.

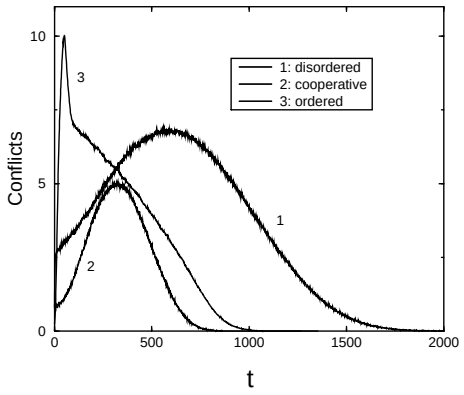


FIG. 23: Number of conflicts in dependence of the time for all three regimes; $\rho = 0.03$ and $\mu = 0$.

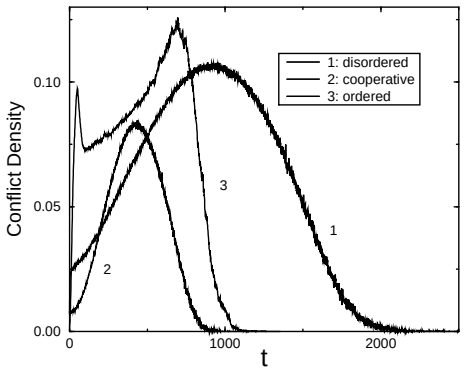


FIG. 24: Same as fig. 21, but for $\rho = 0.03$ and $\mu = 0.9$.

Figs. 23 and 24 show the number of conflicts and the conflict density during an evacuation for the density $\rho = 0.03$ and $\mu = 0.9$. Since there are now less particles in the system, they will not meet each other that often in the disordered and cooperative regime. For times smaller than the evacuation time of the ordered regime the number of conflicts and the conflict density are largest in the ordered regime, where all particles are packed in a small region near the exit.

### F. Column in front of the exit

As an example for safety estimations in architectural planning we investigate how evacuation times change if a column (i.e. a non-traversable obstacle) is placed in front of the exit. The authors of [5, 6], who studied the same situation and found surprising results, called for complementary data from experiments or other models to confirm their findings. We therefore study the scenarios of [5, 6] in the following.

Fig. 25 shows a mid time stage of evacuations for a column placed central in front of the exit. The size of the column is $3 \times 3$ cells. It is placed within a distance of one cell from the door. We compare with situations

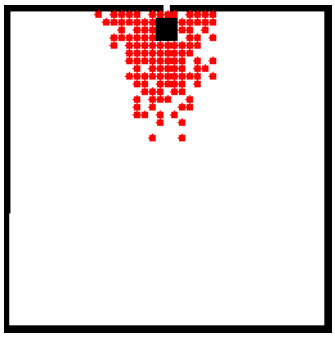

FIG. 25: Mid time configuration of an evacuation of a room with one door at the middle of the top wall with an additional column of size $3 \times 3$ cells placed in front of it. The width of the door is one cell.

where this column has been shifted (to the left or right) parallel to the exit by one or two lattice sites. Our focus is on the ordered regime where friction effects are strongest. The static floor fields $S$ used in the simulations have been calculated using a Manhattan metric (for details see [20]). Fig. 26 shows the averaged evacuation times as a function of the friction parameter $\mu$ for a room with different configurations of the column. The placing of the column does not influence the evacuation times for $\mu = 0$. Here the movement is nearly deterministic and the particles do not hinder each other. For higher values of $\mu$ the column becomes more and more relevant. It causes a subdivision of the crowd and decreases the local pressure between the particles. Therefore the evacuation times become smaller. They are minimized for a column placed in a slightly asymmetric configuration in front of the exit (with a shift of one lattice site, fig. 26).

How can this surprising result be understood? On one hand, the column has a certain screening effect that forces some pedestrians to take a detour and therefore potentially increases the evacuation time. On the other hand, the column subdivides the pedestrian flow and so can lead to a reduction of conflict situations, especially close to the exit. The competition between these two effects is then responsible for the nontrivial dependence of the evacuation times on the position of the column.

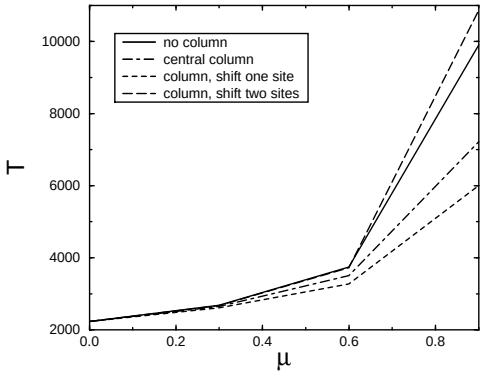


FIG. 26: Evacuation time as function of the friction parameter $\mu$ for four room geometries: no column, central column and column shifted by one and two lattice sites. The initial density is $\rho = 0.3$ and the coupling strengths are $k_S = 10$, $k_D = 0$ corresponding to the ordered regime.

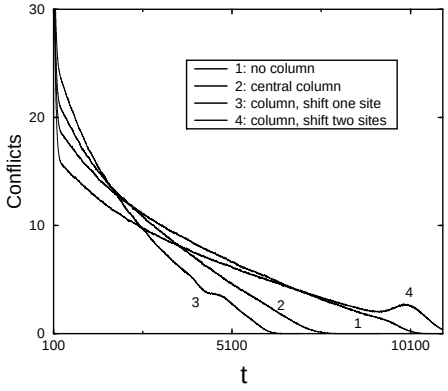


FIG. 27: Number of conflicts for a room with one door compared to various positions of an additional column close to the exit. The friction parameter is $\mu = 0.9$. All other parameters are the same as in fig. 26.

Fig. 27 shows the number of conflicts for three different positions of the column in comparision to a room without column. The evacuation time $T$ is minimal with the column shifted one site (curve 3). In this case, the total number of conflicts during evacuation, which is the integral of the curve, is also minimal. However, in the early stage of the evacuation, the number of conflicts is bigger than for all other cases. This is a result of the subdivision of people in the early stage of the dynamics which occurs most pronounced in case 3. This subdivision enables pedestrians to escape from the room faster than in the other cases since a smoother flow is formed which reduces the evacuation time at the expense of an increasing number of conflicts in the early stage. Furthermore the number of dangerous conflicts close to the door —

which have a direct influence on $T$ (see the discussion in Sec. IV E) — is reduced.

Comparing the cases 2 and 3, the existence of the column reduces the evacuation time in both cases due to the above reason. However, for case 2 of a central column evacuation times are larger than for the shifted one of case 3. In case 2, *all* the people in the room have to avoid the column and take a detour, while for a slightly shifted column some still can reach the exit directly. Thus a central column has a stronger screening effect which leads to the increase of the evacuation time compared to the slightly shifted case. In case 4, the column does not contribute so much to the subdivision of the flow, but acts more like an obstacle. For larger shifts the results will approach those of case 1.

## V. CONCLUSIONS

We have extended a recently introduced stochastic cellular automaton for pedestrian dynamics by incorporating friction effects. These are closely related to the occurance of conflicts, i.e. situations where several people try to occupy the same space. Such conflicts are only resolved with probability $1-\mu$, where $\mu$ is called friction parameter. This implies that friction as introduced here does not influence the motion of a single pedestrian (e.g. by reducing her average speed), but appears only through interactions. Friction effects become important in situations where locally high density regions occur. It therefore can have a strong impact on global quantities like evacuation times although it acts only locally.

To elucidate friction effects and the role of conflicts we have investigated a simple evacuation scenario, especially the evacuation time and the time evolution of the process. Without friction three different regimes with different behaviour can be distinguished, as shown in [17]. Introducing $\mu > 0$ affects these regimes in a different way.

In general, the ordered regime, characterized by strong coupling to the static field and weak coupling to the dynamic field, is affected most. This is not surprising since for sufficiently large initial densities large queues are formed at exits and clogging becomes relevant. The introduction of friction leads to a strong increase of the evacuation time (fig. 6) due to a strong increase of conflicts (figs. 19, 20). Here it is important that the conflicts occur mainly very close to the exit and thus have an immediate influence on the outflow. In contrast, in the other regimes conflicts typically occur everywhere in the system and have therefore a weaker influence on the outflow properties.

Apart form evacuation times we have also investigated the time evolution of an evacuation process. After the introduction of friction the outflow is irregular with periods of stucking. This leads to plateaus in the number $\langle N(t)\rangle$ of evacuated persons after time $t$ very similar to the behaviour observed in granular flow [7, 8, 9, 10, 11, 12, 13]. Here the formation and breaking of arches is responsible for the irregular flow. Similar in our case friction is responsible for the formation of arch-like structures that block the flow close to the door. The plateaus occur randomly and can therefore not be seen after averaging over different samples. The averaged $N(t)$-curves typically show a linear behaviour. Using simple combinatorial arguments we found $N(t) \sim \frac{1-\mu}{2-\mu} \cdot t$ for the $\mu$-dependence of the asymptotic behaviour of the number of evacutated persons. This expression agrees quite well with the numerical data for densities not too small up to intermediate values of $\mu$.

Finally we have shown in Sec. IV F that the introduction of friction is essential to reproduce the surprising effects observed in [6] when placing an additional column in front of the exit. As in [6] this column does not necessarily act as an obstacle, but can — under certain conditions, e.g. a slightly asymmetric position — improve evacuation times considerably. The fact that the model used here differs in many respects from the social-force model [21] (e.g. sign and type of interactions) used in [6] implies a certain robustness of this phenomenon.

### Acknowledgments

We like to thank H. Klüpfel, F. Zielen, A. Kemper and D. Helbing for useful discussions.

## APPENDIX A

Defining the function

$$a(t) = \sum_{n=0}^{[t/2]} \binom{t-n}{n} z^n, \tag{A1}$$

we have

$$\begin{aligned} a(t) &= 1 + \sum_{n=1}^{[t/2]} \left[ \binom{t-n-1}{n} + \binom{t-n-1}{n-1} \right] z^n \\ &= \sum_{n=0}^{[t/2]} \binom{t-n-1}{n} z^n + \sum_{n=1}^{[t/2]} \binom{t-n-1}{n-1} z^n. \end{aligned} \tag{A2}$$

The first term of the r.h.s in (A2) can be rewritten as

$$\sum_{n=0}^{[(t-1)/2]} \binom{t-n-1}{n} z^n = a(t-1). \tag{A3}$$

For odd $t$ this is obvious since then $[(t-1)/2] = [t/2]$. For even $t$ we have $[(t-1)/2] = [t/2] - 1$, but the additional term in the sum vanishes.

The second term of the r.h.s in (A2) becomes

$$z \sum_{n=0}^{[(t-2)/2]} \binom{t-n-2}{n} z^n = z a(t-2). \tag{A4}$$

Thus we obtain the recursive relation

$$a(t) = a(t-1) + za(t-2). \tag{A5}$$

The solution of this recursion for $a(0) = a(1) = 1$ is given by

$$a(t) = \frac{1}{\sqrt{1+4z}} \left[ x_+^{t+1} - x_-^{t+1} \right] \tag{A6}$$

where $x_\pm$ are the roots of the quadratic equation $x^2 - x - z = 0$, i.e.

$$x_\pm = \frac{1 \pm \sqrt{1+4z}}{2}. \tag{A7}$$

Therefore we have

$$\sum_{n=0}^{[t/2]} \left( \begin{array}{c} t-n \\ n \end{array} \right) z^n = \frac{1}{\sqrt{1+4z}} \left[ \left( \frac{1+\sqrt{1+4z}}{2} \right)^{t+1} - \left( \frac{1-\sqrt{1+4z}}{2} \right)^{t+1} \right]. \tag{A8}$$


[1] D. Chowdhury, L. Santen, and A. Schadschneider: Phys. Rep. **329**, 199 (2000)
[2] D. Helbing: Rev. Mod. Phys. **73**, 1067 (2001)
[3] T. Nagatani: Rep. Prog. Phys. **65**, 1331 (2002)
[4] M. Schreckenberg and S.D. Sharma (Ed.): *Pedestrian and Evacuation Dynamics* (Springer 2001)
[5] D. Helbing, I. Farkas, P. Molnar, and T. Vicsek: in [4], p. 21
[6] D. Helbing, I. Farkas and T. Vicsek: Nature **407**, 487 (2000)
[7] D.E. Wolf, P. Grassberger, (Ed.): *Friction, Arching, Contact Dynamics*, World Scientific 1997
[8] M. Nicodemi: Phys. Rev. Lett. **80**, 1340 (1998)
[9] O. Moriyama, N. Kuroiwa, M. Matsushita, and H. Hayakawa: Phys. Rev. Lett. **80**, 2833 (1998)
[10] S. McNamara and W.R. Young: Phys. Fluids A**4**, 496 (1992)
[11] G.H. Ristow and H.J. Herrmann: Phys. Rev. **E50**, R5 (1994)
[12] S. Horlück and P. Dimon: Phys. Rev. **E60**, 671 (1999)
[13] S.S. Manna and H.J. Herrmann: Eur. Phys. J. **E1**, 341 (2000)
[14] C. Burstedde, K. Klauck, A. Schadschneider, and J. Zittartz: Physica **A295**, 507 (2001)
[15] A. Schadschneider: in [4], p. 75
[16] C. Burstedde, A. Kirchner, K. Klauck, A. Schadschneider, and J. Zittartz: in [4], p. 87
[17] A. Kirchner and A. Schadschneider: Physica **A312**, 260 (2002)
[18] E. Ben-Jacob: Contemp. Phys. **38**, 205 (1997)
[19] D. Chowdhury, V. Guttal, K. Nishinari, and A. Schadschneider: J. Phys. **A** (in press)
[20] A. Kirchner: *Modellierung und statistische Physik biologischer und sozialer Systeme*, Dissertation, Universität zu Köln (2002); available for download at `http://www.thp.uni-koeln.de/~aki`
[21] D. Helbing and P. Molnar: Phys. Rev. **E51**, 4282 (1995)
[22] This regime has been denoted as 'optimal regime' in [17].
[23] In reality, pushing and shoving will occur. Since no motion is possible in the jammed states of our model, this is neglected here. It can, however, be incorporated in a more sophisticated version of the model which e.g. allows to determine the pressure exerted by the pedestrians.